fluorinated hydrocarbon and noting that the degree of halogenation increases in going from Propellant 152a to 142b to 114 or 12.

To determine the relative stability of the prepared epinephrine salts compared to epinephrine bitartrate, several formulations were prepared and studied over a 60-day period. Based upon the results of the solubility study, it was decided to formulate several aerosol preparations by suspending the salt in the propellant. Since epinephrine bitartrate is slightly soluble in alcohol, those formulations containing alcohol (Formulations A and B) would have some of the epinephrine salt in partial solution. The other formulations contain the salt in suspension. The former formulations were prepared so that some indication of the stability of the salt in solution could be obtained. The results gained from this study of the epinephrine salts in various aerosol formulations indicate that the decomposition taking place under these conditions can be treated as first order. This finding can be noted in Figs. 1–4 where a straight line resulted from a plot of log concentration *versus* time.

Of all the salts studied, epinephrine bitartrate and maleate seem to be the most stable under the conditions of this study. It was also noted that sodium bisulfite, present as an antioxidant, had a tendency to reduce the rate of decomposition as compared to ascorbic acid. No attempt was made to adjust the pH of the solutions but the effect of pH upon the stability of these formulations is currently under study. The presence of ethyl alcohol in the formulation seemed to have very little effect, if any, upon the decomposition of the epinephrine salts. In fact, a comparison of Formulation D, containing only epinephrine salt and propellant, with the other formulations shows very little difference. However, these results might be quite different if extended over a longer period of time. The presence of ethyl alcohol, however, can affect the stability of the dispersion, resulting in agglomeration and caking. The same conclusion can be stated for those formulations containing a surfactant. Additional studies are underway to study more fully the stability of these epinephrine salts, both from a physical and a chemical viewpoint. Of all of the salts studied, epinephrine maleate shows the greatest potential for use in aerosol form and is under further study.

## SUMMARY

Epinephrine maleate, fumarate, and malate were prepared by modification of an existing method. The partition coefficient of these epinephrine salts was determined between octyl alcohol–water and between hexadecyl alcohol–water and found to be similar to the partition coefficient of epinephrine bitartrate. Epinephrine bitartrate and malate were found to be the least soluble in the fluorocarbon propellant while the maleate and fumarate showed a higher degree of solubility in these propellants. The results of the solubility study of these epinephrine salts in the propellants indicated that the formulation of epinephrine salts as an aerosol dosage form must be accomplished through use of a cosolvent or by formulating a dispersion system. From the stabilty study of the epinephrine salts in an aerosol formulation, it was noted that the decomposition which took place followed first-order kinetics and that epinephrine maleate and bitartrate seem to be more stable than the other salts of epinephrine. Further studies are indicated to determine the extent of this stability.

## REFERENCES

(1) W. Brockband and C. D. R. Pengelly, *Lancet*, **1**, 187(1950).

(2) R. W. Monto, J. W. Rebuck, and M. J. Brennan, *Amer. J. Med. Sci.*, **225**, 113(1953).

(3) M. Gelfand and M. A. Shearn, *Proc. Soc. Exp. Biol. Med.*, **8**, 134(1952); through *Chem. Abstr.*, **46**, 8261d(1952).

(4) "The National Formulary," 13th ed., Mack Publishing Co., Easton, Pa., 1970, p. 803.

(5) "Remington's Pharmaceutical Sciences," 14th ed., Mack Publishing Co., Easton, Pa., 1970, p. 887.

(6) W. C. Grater and C. B. Shuey, *J. South. Med. Ass.*, **51**, 1600 (1958).

(7) T. Freedman, *Postgrad. Med.*, **20**, 667(1956).

## ACKNOWLEDGMENTS AND ADDRESSES

Received April 30, 1970, from the *Graduate Division, College of Pharmacy, St. John's University, Jamaica, NY 11432*

Accepted for publication October 21, 1971.

Presented in part to the Aerosol Division, Chemical Specialties Manufacturers Association, Chicago meeting, May 1969.

Abstracted in part from a thesis submitted by Jitendra M. Patel to the Graduate Division, College of Pharmacy, St. John's University, in partial fulfillment of the Master of Science degree requirements.

On the basis of this research project, the 1968 Aerosol Research Award of the Chemical Specialties Manufacturers Association was presented to Jitendra M. Patel.

▲ To whom inquiries should be directed.

# Dissolution Rate Patterns of Log-Normally Distributed Powders

**J. THURØ CARSTENSEN▲ and MAHMOUD N. MUSA**

**Abstract** □ Particles dissolving in a dissolution medium initially decrease in linear dimension, while the number of particles remains unaltered. At a particular point in time ($t_c$) the smallest particle disappears, and from that point on the number of particles decreases. These phenomena were simulated on a digital computer, and the agglomerate dissolution pattern under sink conditions was shown to follow a cube root law, but the slopes differ according to whether $t < t_c$ or $t > t_c$.

**Keyphrases** □ Dissolution rates—patterns of log-normally distributed powders □ Powders, dissolution under sink conditions—rate patterns, (approximate) numerical solution of log-normal distribution integrals □ Computer simulations—particle dissolution, disappearance □ Particle dissolution, sink conditions—powder, log-normal distribution, rate patterns, computer simulation

Rates of dissolution and the mechanisms involved in the dissolution process have been the subjects of large volumes of literature in the last decade. The importance of dissolution rates in biopharmaceutics is manifested by the official methods for dissolution rate testing recently adopted by the USP and the NF.

Table I—Means and Standard Deviations of the Log-Normal Distributions Employed and Slopes of the Cube Root Treatments of the Data

| Log $\mu$, $\mu$ in Microns | $\sigma$ | Slope $\tau < \tau_c$ | Slope $\tau > \tau_c$ | Log $\mu$, $\mu$ in Microns | $\sigma$ | Slope $\tau < \tau_c$ | Slope $\tau > \tau_c$ |
|---|---|---|---|---|---|---|---|
| 0.69897 | 0.01380 | 0.9251 | 7.86 | 1.34242 | 0.01380 | 0.2102 | 1.78 |
| | 0.02009 | 0.9207 | 5.45 | | 0.02009 | 0.2093 | 1.24 |
| | 0.02639 | 0.9161 | 4.16 | | 0.02639 | 0.2082 | 0.95 |
| | 0.03218 | 0.9125 | 3.45 | | 0.03218 | 0.2074 | 0.78 |
| | 0.03798 | 0.9059 | 2.94 | | 0.03798 | 0.2059 | 0.67 |
| 1.0000 | 0.01380 | 0.4625 | 3.91 | 1.47712 | 0.01380 | 0.1542 | 1.31 |
| | 0.02009 | 0.4604 | 2.72 | | 0.02009 | 0.1535 | 0.91 |
| | 0.02639 | 0.4581 | 2.08 | | 0.02639 | 0.1527 | 0.70 |
| | 0.03218 | 0.4563 | 1.72 | | 0.03218 | 0.1521 | 0.58 |
| | 0.03798 | 0.4530 | 1.47 | | 0.03798 | 0.1510 | 0.49 |
| 1.23045 | 0.01380 | 0.2721 | 2.30 | 1.60206 | 0.01380 | 0.1156 | 0.98 |
| | 0.02009 | 0.2708 | 1.60 | | 0.02009 | 0.1151 | 0.68 |
| | 0.02639 | 0.2694 | 1.23 | | 0.02639 | 0.1145 | 0.52 |
| | 0.03218 | 0.2684 | 1.02 | | 0.03218 | 0.1141 | 0.43 |
| | 0.03798 | 0.2664 | 0.87 | | 0.03798 | 0.1132 | 0.37 |

The principal theoretical considerations in this field were published by Higuchi and Hiestand (1, 2). Their treatment assumes that a steady state is attained in the liquid surrounding the solid particle and that the particle sizes are distributed log-normally; it also takes into account the temporal disappearance of particles from the low distribution tail. The ensuing expressions become analytically unmanageable and integrals are solved by approximation functions, notably substituting $n(a_0) = K/a_0^4$ for the log-normal distribution, where $a_0$ is the initial particle size, $n$ is the fraction of particles, and $K$ is a constant. The function approximates the log-normal oversize distribution over 60% of the particle-size range, and reasonable agreement with experiment is achieved in this manner.

The purpose of the study reported here was to obtain solutions of the integrals not by rigid integration of approximation functions but rather by (approximate) numerical solution of integrals of the actual log-normal distribution. Such work, obviously, is done with the aid of a computer. The Noyes–Whitney equation (3, 4) and the ensuing Hixson and Crowell equation (5) were employed here as vantage points for the treatment.

Many authors (6–11) showed that particles prepared by procedures such as milling and grinding (6) and precipitation (11), which are based on random processes, produced skewed distribution functions close to log-normal. It is assumed in the following discussion that the powder dissolving is of such a log-normal distribution.

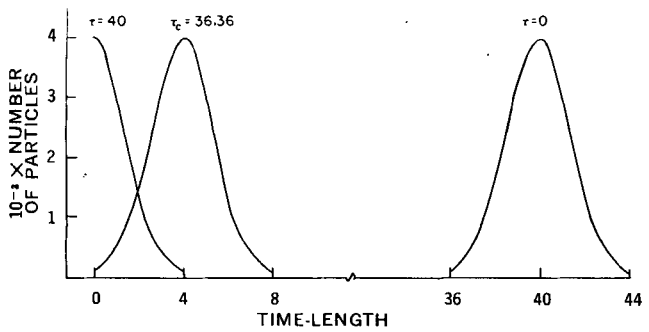


**Figure 1**—*An example of particle-size distributions at various times during the dissolution process. The ordinate is number of particles; the original number of particles is 10,000 at a "mean" diameter of 40 μ; the smallest diameter is $\tau_c$ = 36.36 and the largest is Q = 44.00 μ. At time-length 36.36, there is still the same number of particles but the "mean" diameter is now 3.64 μ. At time-length 40, half of the particles have disappeared.*

## THEORETICAL

If the Noyes–Whitney treatment (3, 4) is applied under the assumption of perfect sink conditions, then:

$$\frac{dw_i}{dt} = -D \cdot \pi \cdot a_i^2 \cdot C_s \qquad \text{(Eq. 1)}$$

where $w$ is the amount by weight [*i.e.*, $-(dw/dt)$ is the decrease in weight per unit time], $D$ is the diffusion rate constant, $a$ is the "diameter," and $C_s$ is the saturation concentration of the substance in the dissolution medium. The assumption is made that the particles are spherical, but any shape that retains its shape factor during the dissolution process gives rise to, basically, the same equations developed here. The subscripts $i$ in Eq. 1 refer to the fraction $dN_i/N$ of the solid which has diameters in the range $a_i$ to $a_i + da_i$, $N$ being the total number of particles.

Further assumptions inherent in this treatment are that: (*a*) the particles dissolve in isotropic fashion, and (*b*) the solubility is the same for particles of all sizes. The latter, of course, is not correct; in particular, the very fine (less than micron size) fraction of the powder sample has considerably higher solubility than the coarser cuts. Higuchi and Hiestand (1, 2) discussed some of the effects of this on dissolution rate patterns.

Table II—Number of Particles and Percent of Weight (Volume) Undissolved as a Function of Time-Length for a Particle-Size Distribution with Geometric Mean 40 (log $\mu$ = 1.60206) and Standard Deviation $\sigma$ = 0.0138

| Before Critical Time-Length: Time | Number of Particles | Percent of Weight Undissolved | After Critical Time-Length: Time | Number of Particles |
|---|---|---|---|---|
| 0 | 10,000 | 100. | 36.36 | 10,000 |
| 3.63 | 10,000 | 75 | 36.99 | 9,931 |
| 7.27 | 10,000 | 59 | 38.06 | 9,370 |
| 10.91 | 10,000 | 39 | 39.02 | 7,728 |
| 14.55 | 10,000 | 26 | 40.53 | 3,249 |
| 18.18 | 10,000 | 16 | 41.47 | 1,191 |
| 21.82 | 10,000 | 9.5 | 42.19 | 413 |
| 25.45 | 10,000 | 4.9 | 43.50 | 7 |
| 29.09 | 10,000 | 2.1 | 44.00 | 0 |
| 32.72 | 10,000 | 0.66 | | |

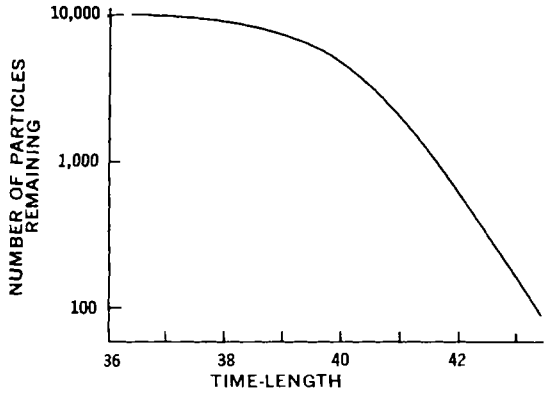


**Figure 2**—*Number of particles as a function of time-length beyond the critical time-length. Data from Table II.*

Weight and diameter are related by $w_i = \pi \cdot a_i^3 \cdot \rho/6$, so $dw_i/dt = (\pi/2) \cdot a_i^2 \cdot \rho \cdot da_i/dt$; this inserted in Eq. 1 yields: $da_i/dt = -2 \cdot D \cdot C_s/\rho$ which integrates to:

$$a_i = a_i^0 - [2 \cdot D \cdot C_s/\rho] \cdot t \qquad \text{(Eq. 2)}$$

It is noted that $a_i$, with the assumptions made, is independent of particle-size distributions.

Inserting Eq. 2 and the weight-diameter relation into Eq. 1 yields the well-known cube root law:

$$w_i = \frac{\pi \cdot \rho}{6} \cdot [a_i^0 - (2 \cdot D \cdot C_s/\rho) \cdot t]^3 \qquad \text{(Eq. 3)}$$

Since at time $t = 0$, $w_i^0 = (\pi \cdot \rho/6) \cdot (a_i^0)^3$, Eq. 3 may be rewritten:

$$w_i^{0\,1/3} - w_i^{1/3} = [\pi \cdot \rho/6]^{1/3} \cdot [2 \cdot D \cdot C_s/\rho] \cdot t \qquad \text{(Eq. 4)}$$

This derivation (aside from nomenclature) follows fairly closely that of other authors (5).

In the following discussion, the term $\tau = [2 \cdot D \cdot C_s/\rho] \cdot t$ is used as a measure of time and is denoted as time-length (since it does not have a time dimension). If the smallest diameter in the powder sample is $a_s^0$, then Eq. 3 (as well as Eq. 4) holds for $t < a_s^0 \cdot \rho/2 \cdot D \cdot C_s$. At the critical time, $t_c = a_s^0 \cdot \rho/2 \cdot D \cdot C_s$ (*i.e.*, $\tau_c = a_s^0$); at higher times the number of particles decreases.

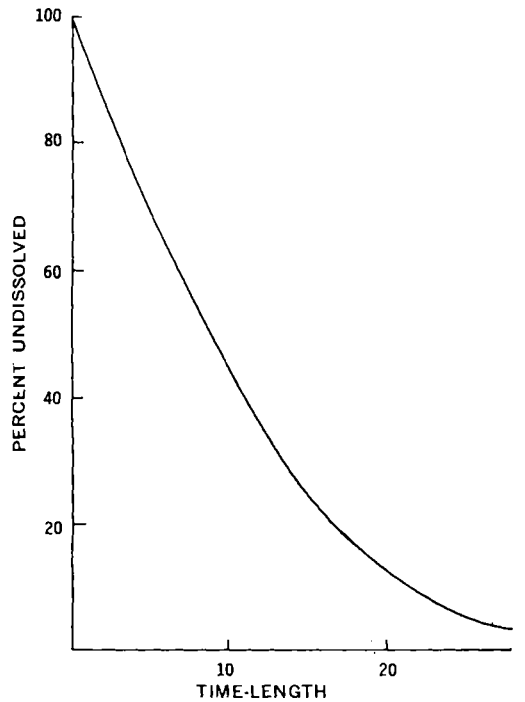


**Figure 3**—*Amount undissolved as a function of time-length in the period prior to the critical time-length. The geometric mean is 40 μ, and the standard deviation of the log-normal distribution is σ = 0.0138.*

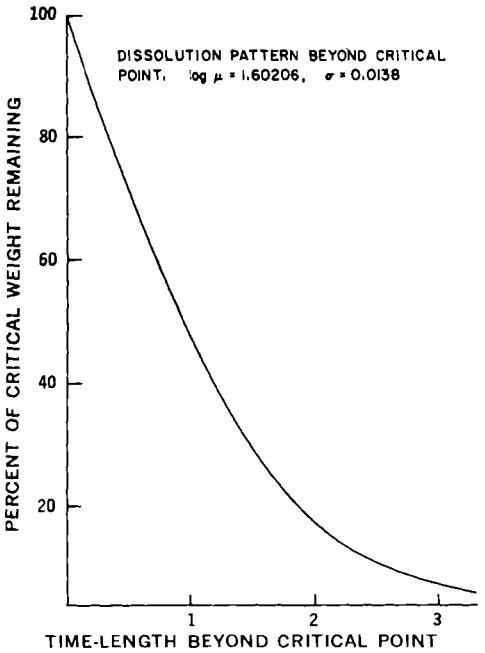


**Figure 4**—*Amount undissolved expressed as percent of the amount present at the critical time-length. The period covered is that subsequent to the critical time-length. The geometric mean is 40 μ originally, and the standard deviation of the log-normal distribution is σ = 0.0138.*

## EXPERIMENTAL

Log-normal (number) distributions were generated on a computer[1] for the 30 particle-size distributions shown in Table I. A log-normal particle-size distribution is given by:

$$Pr(a) = \frac{1}{\sigma \cdot \sqrt{2\pi}} \cdot \exp\,[-(\log \mu - \log a)^2/2 \cdot \sigma^2] \qquad \text{(Eq. 5)}$$

where $\log \mu$ is the logarithmic mean, $\sigma$ is the standard deviation, and $Pr(a)$ is the fractional frequency (probability) at diameter $a$. The function is normalized (*via* the preexponential factor) so that $\int_{-\infty}^{\infty} Pr(a)da = 1$; *i.e.*, all values of $a$ are possible. In a realistic situation, however, there are maximum and minimum diameters at zero time ($Q$ and $\tau_c$, respectively). If these are taken at $\pm 3\sigma$ (*i.e.*, if $Q$ is given by $\log Q - \log \mu = \log \mu - \log \tau_c = 3\sigma$), then $\int_{-\infty}^{\infty} Pr(a)da = 0.9974$, so employing the concept of maximum and minimum diameters at $\pm 3\sigma$ inflicts only a small overall error.

According to Eq. 2, the diameter decreases linearly in time. At any time length $\tau < \tau_c$, the number distribution is identical to that at zero time, but all diameters are smaller than the original by $\tau$. In the initial stage, the weight fraction remaining undissolved then is:

$$\frac{\pi \cdot \rho/6}{w_0 \cdot \rho \cdot \sqrt{2\pi}} \cdot \int_{\tau_c - \tau}^{Q - \tau} (a^0 - \tau)^3 \cdot \Phi(\tau) d(a^0 - \tau) \qquad \text{(Eq. 6)}$$

where $\Phi(\tau) = \exp\,[-\{\log(\mu - \tau) - \log(a^0 - \tau)\}^2/2 \cdot \sigma^2]$, and $a^0$ refers to initial diameters. This integral is evaluated at time-lengths $0.1\tau_c, 0.2\tau_c, \ldots, 0.9\tau_c$ by computer. The evaluation of the integral is performed by dividing the $3\sigma$-interval into 100 intervals and computing the area of the ensuing histogram.

[1] Univac model 1108.

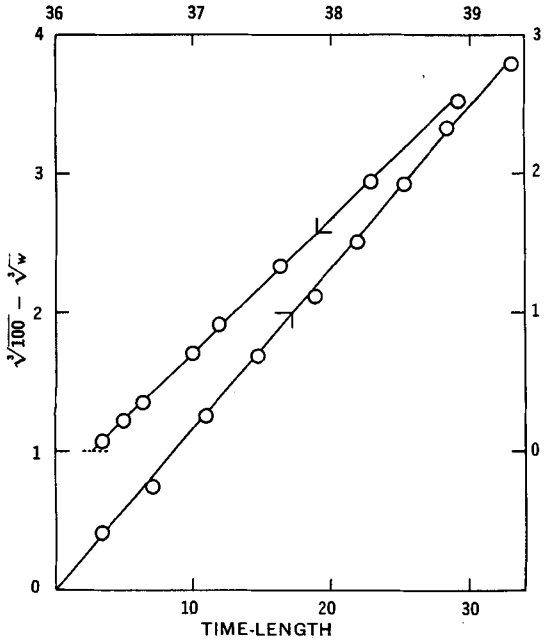


**Figure 5**—*Data from Figs. 3 and 4 expressed in the form of cube root relations. The initial amount is set at 100, so that* w *denotes percent undissolved.*

Once the critical time-length, $\tau_c$, is reached, the number of particles decreases. The weight fraction remaining undissolved at any time-length $\tau > \tau_c$ is given by the same integral as in Eq. 6, except the lower limit is now zero. The low tail of the distribution has been truncated in this expression. The situation is best depicted graphically as in Fig. 1, where the distribution is expressed as the

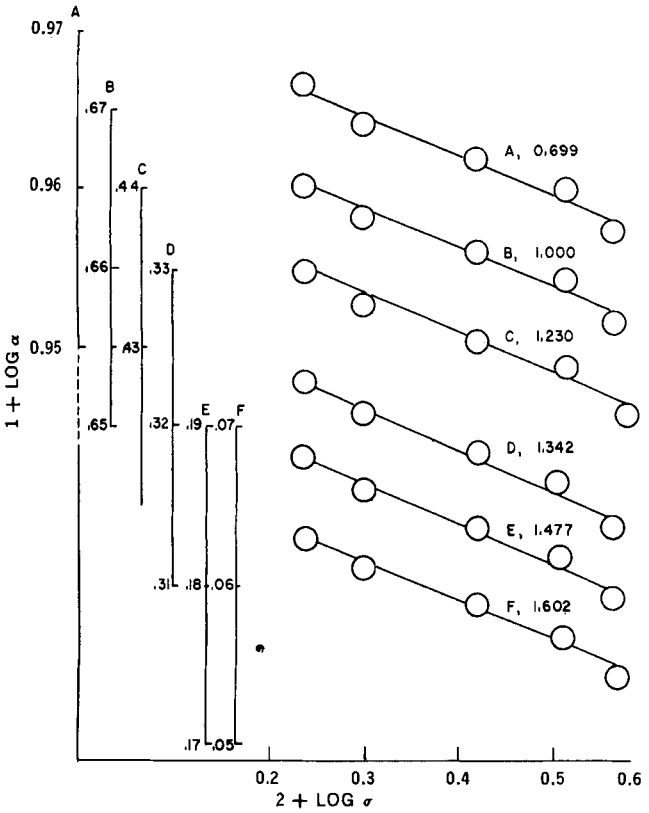


**Figure 6**—*Slopes* ($\alpha$) *of lines of the type shown in Fig. 5 prior to the critical time-length. The slopes are shown as a function of the standard deviation of the particle-size distribution in a log–log fashion.*

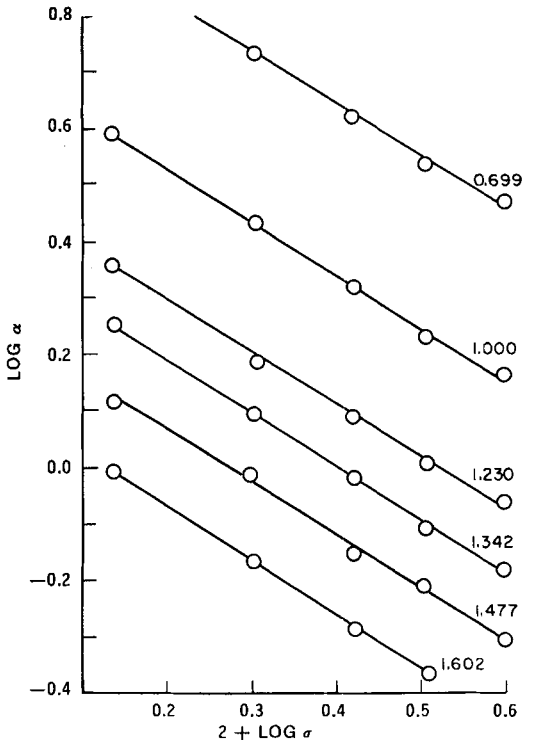


**Figure 7**—*Graph similar to Fig. 6 for data at time-lengths beyond the critical time-length.*

number of particles in a population of 10,000, as a function of diameter at $\tau = 0$, $\tau = \tau_c$, and $\tau > \tau_c$.

To arrive at possible functional relationships, the analysis of the curves is broken down in the following into two parts: (*a*) data at $\tau < \tau_c$, and (*b*) data subsequent to $\tau_c$. In the latter case, the weights (or volumes) are related to that at time $\tau = \tau_c$; *i.e.*, the function:

$$\frac{w(\tau)}{w(\tau_c)} = \int_0^{Q-\tau} \Phi(\tau)d(a^0 - \tau) \Big/ \int_0^{Q-\tau_c} \Phi(\tau)d(a^0 - \tau) \quad \text{(Eq. 7)}$$

is evaluated as a function of $\tau$. The function cannot be obtained in closed form and, as before, the integrals are evaluated by computer

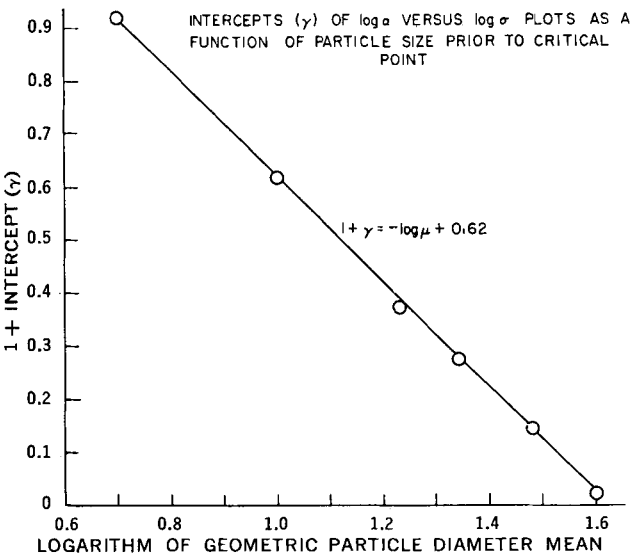


**Figure 8**—*Intercepts of lines shown in Fig. 6 as a function of the logarithm of the standard deviation of the particle-size distribution;* $\tau < \tau_c$.

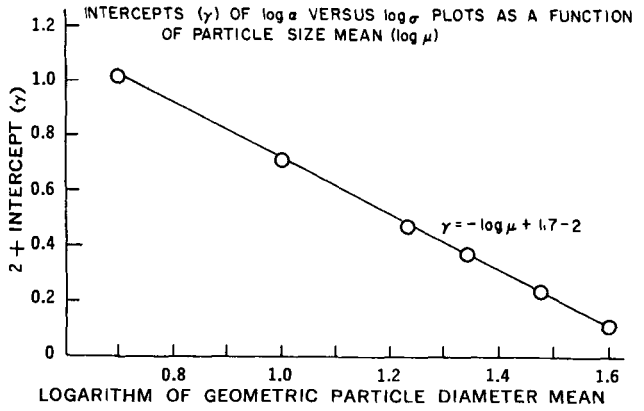


**Figure 9**—*Intercepts of lines shown in Fig. 7 as a function of the logarithm of the standard deviation of the particle-size distribution;* $\tau > \tau_c$.

by dividing the $\pm 3\sigma$-interval into 100 intervals and using the areas of the ensuing histograms. The histograms in the numerator consist of 100, 99, 98, . . . , 1 areas as the expression is evaluated at time-lengths $\tau_c$, $(0.99\tau_c + 0.01Q)$, $(0.98\tau_c + 0.02Q)$, . . . , $(0.01\tau_c + 0.99Q)$.

## RESULTS

A typical example of the number of particles as a function of time-length beyond the critical time-length is shown in Table II and Fig. 2. All the solutions generated by computer have graphical presentations of the form shown in Figs. 3 and 4. The former is an example of the situation prior to the critical time-length, and the latter exemplifies the situation after the critical time-length. A combination of the two is an example of the entire curve which, of course, shows a (not necessarily very noticeable) elbow at the critical time. Attempts to linearize both parts of the curve by plotting $\log (w/w^0)$ as a function of $\tau$ or by probit function as proposed by Wood (12) are not successful in the framework of the assumptions made here. If the data are plotted by cube root treatment (Eq. 4), linearity results (Fig. 5). The slopes ($\alpha$), of course, no longer have the meaning implied in Eq. 4. The slopes are a function of the standard deviation of the particle-size distributions and are listed in Table I, both for $\tau < \tau_c$ and $\tau > \tau_c$. The slopes in both time-length periods are logarithmically related to the standard deviations (Figs. 6 and 7).

It is noted from Figs. 6 and 7 that (as expected) the slopes are independent of the particle-size average. The intercepts ($\gamma$), however, are dependent on particle size, and they appear to be proportional to the logarithm of the geometric mean (*i.e.*, the average of $\log a^0$) as shown in Figs. 8 and 9; here, again, each figure represents one type of time-length period ($\tau < \tau_c$ and $\tau > \tau_c$).

By employing best fits for the lines in Figs. 6 and 8, the following relations ensue: $\log \alpha = -1.05 \cdot \log \sigma - \log \mu + 1.7$, so that $\alpha = 50/(\sigma^{1.05} \cdot \mu)$ and:

$$w^{0\,1/3} - w^{1/3} = [50/(\sigma^{1.05} \cdot \mu)] \cdot \tau = \frac{100 \cdot D \cdot C_s}{\sigma^{1.05} \cdot \mu \cdot \rho} \cdot t \quad \text{(Eq. 8)}$$

for the time period prior to the critical point, and by similar treatment of the data in Figs. 7 and 9:

$$w^{0\,1/3} - w^{1/3} = \frac{0.834}{\sigma^{0.025} \cdot \mu} \cdot \frac{D \cdot C_s}{\rho} \cdot t \quad \text{(Eq. 9)}$$

for the time period subsequent to the critical point.

Equations 8 and 9 together describe the general dissolution pattern for the log-normally distributed particle-size population when the particle dissolves isotropically and particle size–solubility relations are neglected.

## REFERENCES

(1) W. I. Higuchi and E. N. Hiestand, *J. Pharm. Sci.*, **52**, 67(1963).

(2) W. I. Higuchi, E. L. Rowe, and E. N. Hiestand, *ibid.*, **52**, 162(1963).

(3) A. Noyes and W. Whitney, *J. Amer. Chem. Soc.*, **19**, 930(1897).

(4) A. Noyes and W. Whitney, *Z. Phys. Chem.*, **23**, 689(1897).

(5) A. Hixson and J. Crowell, *Ind. Eng. Chem.*, **23**, 923(1931).

(6) G. Herdan and M. L. Smith, "Small Particle Statistics," Elsevier, New York, N. Y., 1953.

(7) R. S. Tipson, in "Technique of Organic Chemistry," vol. III, part I, A. Weissberger, Ed., Interscience, New York, N. Y., 1956, p. 431; J. C. Kapteyn and M. J. van Uven, "Skew Frequency Curves in Biology and Statistics," Hoitsema, Grönigen, The Netherlands, 1916.

(8) M. J. van Uven, *Proc. Kon. Ned. Akad. Wetensch.*, **19**, 533(1916).

(9) R. P. Loveland and A. P. H. Trivelli, *J. Franklin Inst.*, **204**, 193, 377(1927).

(10) T. Hatch and S. P. Choate, *ibid.*, **207**, 369(1929).

(11) G. L. Beyer, in "Technique of Organic Chemistry," vol. I, part I, A. Weissberger, Ed., Interscience, New York, N. Y., 1959, p. 197.

(12) J. H. Wood, "*In Vitro* Evaluation of the Release from Dosage Forms," Industrial Pharmacy Section, APhA Academy of Pharmaceutical Sciences, Dallas meeting, Apr. 1966.

## ACKNOWLEDGMENTS AND ADDRESSES

Received August 18, 1971, from the *School of Pharmacy, University of Wisconsin, Madison, WI 53706*

Accepted for publication November 1, 1971.

Presented at the Eleventh Annual Conference on Pharmaceutical Analysis, Land O'Lakes, Wis., 1971.

▲ To whom inquiries should be directed.